

PAPER • OPEN ACCESS

## If there is dissipation the particle can gain energy

To cite this article: R Egydio de Carvalho 2015 *J. Phys.: Conf. Ser.* **641** 012015

View the [article online](#) for updates and enhancements.

### Related content

- [ON VARIABLE 39 IN IC 1613](#)  
J. L. Hutchinson
- [IN 1903](#)  
Harold D. Babcock
- [Coulomb Effect on Inelastic Scattering of Proton on Deformed Nuclei at High Energies](#)  
Zhang Yu-shun



**IOP | ebooks™**

Bringing you innovative digital publishing with leading voices to create your essential collection of books in STEM research.

Start exploring the collection - download the first chapter of every title for free.

# If there is dissipation the particle can gain energy

**R Egydio de Carvalho**

Universidade Estadual Paulista-UNESP – Rio Claro-SP, Brazil

E-mail: [regydio@rc.unesp.br](mailto:regydio@rc.unesp.br)

**Abstract.** In this work, we summarize two different mechanisms to gain energy from the presence of dissipation in a time-dependent non-linear system. The particles can gain energy, in the average, from two different scenarios: i) for very weak dissipation with the creation of an attractor with high velocity, and ii) in the opposite limit, for very strong dissipation, the particles can also gain energy from a boundary crisis. From the thermodynamic viewpoint both results are totally acceptable.

## 1. Introduction

Dissipation, generically, corresponds to a process that consumes energy in such way the particles of the system lose energy until stabilizing in a stable configuration. A typical stable configuration for a dissipative system corresponds to an attractor. However, depending on the structures of the phase space the results can be different of the common sense.

In a chaotic region of a Hamiltonian system [1], a particle can experiment different velocities in the phase space. When this chaotic region is limited by invariant tori, a half of the height of the column of chaos gives approximately the mean velocity of the particles moving in the chaotic sea. If in the superior limit of the column of chaos there is an island of resonance, then the elliptic fixed point from the inside of the island will play a key role in the limit of weak dissipation. On the other hand, for strong dissipation, the coexistence of a point attractor with a chaotic attractor may lead to the crossing of the stable and unstable manifolds of the point attractor, as the parameter of dissipation is varied. This defines a boundary crisis [2] which destroys the chaotic attractor and drives the trajectories, which were in the chaotic attractor, toward the point attractor. These mechanisms are quite different but both allow the particle to receive part of the energy that would be lost and, in the average, an ensemble of particles can attain higher energies than they had without dissipation. The paper is organized as follows, in section 2 we present the model, the results are shown in section 3 and in section 4 the reader will find the conclusion.

## 2. The breathing annular billiard

The model we consider is the annular billiard with periodic time-dependent boundaries. However, before introducing it we present the main aspects of the static annular billiard. This is defined by the annulus between two circumferences, which may be concentric or eccentric. The annulus is free of potential and is the only accessible space for the particles. The outer radius is set equal to 1; the inner one we call by  $r_0$  and the distance between both centers, the eccentricity, we call by  $\delta$ .



For the static case, the particle energy is conserved and the dynamics of a particle moving in the annulus is completely described by the coordinates of a collision with the external boundary. These coordinates are: i) the incidence angle,  $\alpha$ , that the trajectory makes with the normal of the external circle and ii) the angle,  $\theta$ , that the normal makes with the abscissa axis. The corresponding phase space is defined by the variables,  $S = \sin(\alpha)$  and  $L = \theta/2\pi$  in such way that  $S \in [-1, 1]$  and  $L \in [-\frac{1}{2}, \frac{1}{2}]$ .

We call this plane as geometric phase space. There is an auxiliary circumference, with radius  $(r + \delta)$  called caustic, that allows us distinguish a class of trajectories. The trajectories that never cross the caustic are called whispering gallery orbits (WGO) and they correspond to preserving angular momentum motions. The dynamics is governed by two maps: i) one called A-motion, corresponding to the case in which between two consecutive hits with the external boundary, the trajectory does not hit the internal one, and ii) another called B-motion, in which the trajectory collides with the internal circumference before hitting the external one. For the static and concentric geometry, besides the energy, the angular momentum is always conserved, in such way the system is globally integrable. However, for the eccentric geometry, the B-motion implies in no conservation of the angular momentum anymore and chaos appears and grows with the eccentricity.  $\delta$  plays the role of perturbation parameter, as it increases the destruction of invariant tori in the geometric phase space also increases, up the numerical limit  $\delta \approx 3r$ . A more detailed discussion on the static annular billiard can be found in [3-4].

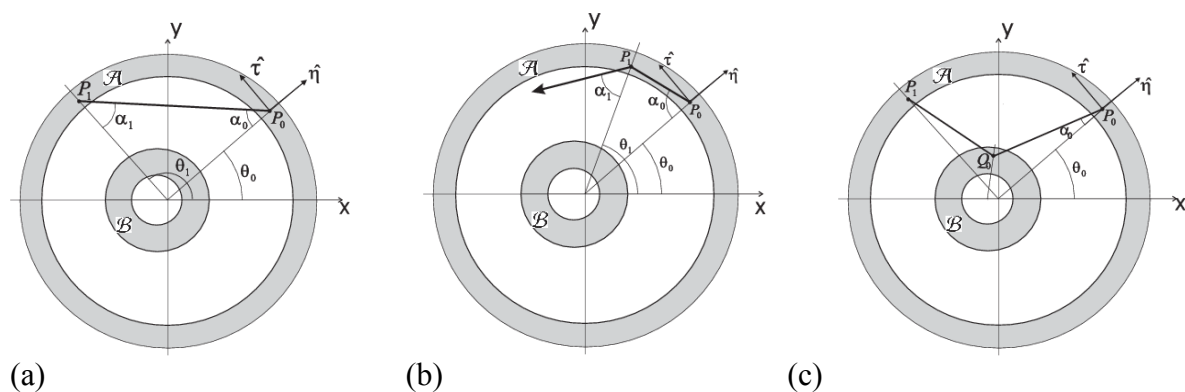
In order to study how a particle can vary its energy we must introduce a time-dependent perturbation. However, to observe confined motions, we need to preserve a global constant of motion; in this case the constant is the angular momentum. So, we will consider the concentric billiard but with both boundaries periodically breathing in time. We define the ratio between both frequencies of oscillation by  $\omega$ . The amplitudes of oscillation and the phases are  $(\varepsilon_R, \varphi)$  and  $(\varepsilon_r, \phi)$  for the outer and inner boundaries respectively. During a collision, the boundaries are not necessarily in the same positions they were in the static case, they have new radii given by  $R(t) = 1 + \varepsilon_R \cos(t + \varphi)$  and  $r(t) = r_0 + \varepsilon_r \cos(\omega t + \phi)$  in such way there are two collision zones in which the particles can suffer collisions. The collision zone associated with the external circumference is the ring  $[1 - \varepsilon_R, 1 + \varepsilon_R]$  while with the internal one it is  $[r_0 - \varepsilon_r, r_0 + \varepsilon_r]$ . Depending on its velocity the particle enters in a collision zone and depending also on the phase of the moving boundary, it may suffer successive collisions before leaving the collision zone. This problem of successive collisions may receive two different approaches. One called complete problem which consider all possibilities of collisions in the algebraic formulation and along the numeric calculations, and another one called simplified problem which keeps the boundaries algebraically static but the momentum of the particle is changed in the instant of the collision as the boundaries were oscillating. Even though there are small differences between both approaches, essentially for low particle velocities, the dynamics are reasonably similar. Hence, to avoid so long cpu-times, the calculations have been done with the simplified description. In this problem, dissipation is introduced through inelastic collisions between the particle and the boundaries. As the breathing corresponds to a radial motion, the tangential component of the particle velocity,  $V_{(n+1)\tau} = V_{(n)\tau}$ , does not change in a collision. On the other hand, the radial component of the particle velocity  $V_\eta$  is given by  $V_{(n+1)\eta} = - \left| -e V_{(n)\eta} + (1+e) \dot{U} \right|$ , where  $(n+1)$  stands for the next collision after the  $n^{\text{th}}$  collision,  $e \in [0, 1]$  is the restitution coefficient and  $U$  is the

velocity of the boundary which is the first derivative of the respective radius,  $\dot{R}(t)$  or  $\dot{r}(t)$ , depending on which boundary the collision occurred. If  $e = 1$  there is no dissipation. A collision is obtained through the intersection between the straight lines of the trajectories with the circumferences with time-dependent radii. Hence, for each collision, with any boundary, the particle changes its radial velocity and we get an iteration of the maps. However, we store only the collisions with the external

boundary. Along this work, the circumferences will be kept concentric. The variation of the energy due to the time-dependent perturbation defines another plane of phase, which we call energy phase plane, defined by the phase of the external boundary  $\varphi$  and the radial particle velocity  $v_\eta$ . The details concerning the algebraic derivation of the non-dissipative maps and the ideas of the dynamics can be found in [5,6] while the introduction of dissipation is detailed in [7,8].

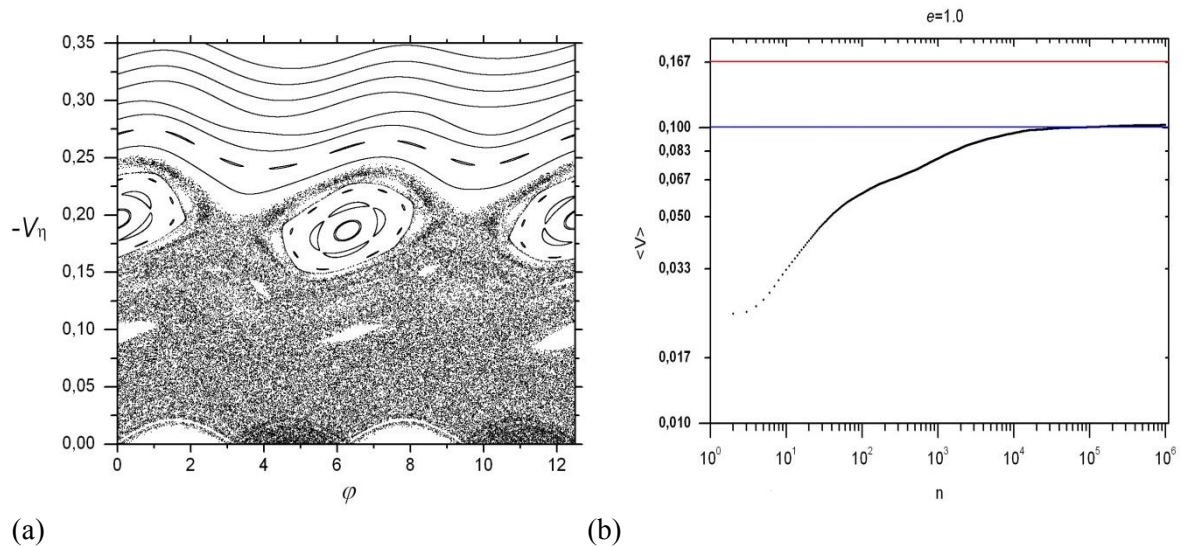
### 3. Discussion and Results

A schematic view of the time-dependent annular billiard is shown in figure (1) in which we see a straight line trajectory suffering a single collision, figure (1a) and successive collisions, figure (1b), in the external collision zone, while in figure (1c) the trajectory goes into the internal boundary before hitting the external one. The particle can also suffer successive collisions in the internal collision zone. Throughout this work we kept  $\delta = 0$  and consider only the concentric case. *Figures (1a), (1b) and (1c) are authorized to be reproduced from Phys. Rev. E73 (2006) 066229, whose DOI is 10.1103/PhysRevE.73.066229, by the American Physical Society through the license number 3607670344906.*



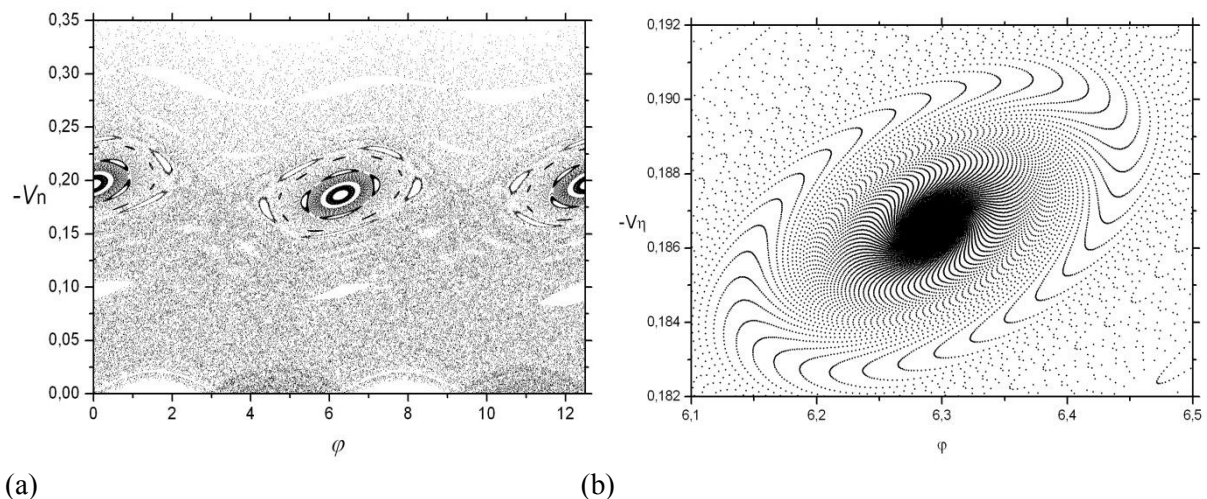
**Figure 1.** Schematic illustrations of the time-dependent annular billiard. The collision zones are the regions denoted by the stylized letters A and B. a) and b) show collisions only with the external collision zone, while in c) it is shown the possibility of also happening collisions in the internal collision zone.

In figure (2) it is presented the energy phase plane for the non-dissipative concentric billiard breathing periodically in time. The set of parameters we used were:  $r_0 = 0.4$ ,  $R = 1$ ,  $\delta = 0$ ,  $e = 1$ ,  $\omega = 0.5$ ,  $\epsilon_R = \epsilon_r = 0.01$  and  $\phi = \pi/4$ . We can observe in figure (2a) that there is a chaotic sea for low velocities and for the velocity  $\sim 0.20$  there is an elliptic fixed point inside the resonance island. Even though there is a thin layer of chaos above the island, we can expect that the mean velocity of an ensemble of particles, starting in the chaotic sea, be approximately  $\langle v \rangle \sim 0.10$ ,  $\sim$  a half of the column of chaos. That is confirmed in figure (2b) where we plotted the mean velocity of an ensemble of 1000 initial conditions starting with  $-v_\eta = 0.02$  and  $\varphi \in [0, 4\pi]$ . After  $10^6$  iterations  $\langle v \rangle$  saturated at  $\sim 0.10$ . *Figures (2a), (2b), (3a), (3b), (3c) and (3d) are authorized to be reproduced from Phys. Rev. E77 (2008) 036204, whose DOI is 10.1103/PhysRevE.77.036204, by the American Physical Society through the license number 3607661418103.*



**Figure 2.** Non-dissipative case. In (a) we see the energy phase plane with invariant tori limiting the growth of the particle velocities, chaos for low velocities and an elliptic fixed point at velocity  $\sim 0.20$ . In (b) we see the behavior of the mean velocity of an ensemble of particles starting in the chaotic sea. It saturates at velocity  $\sim 0.10$ .

In order to analyze the effect of the inelasticity of the boundaries we set a very weak dissipation with  $e = 0.9999$ . In figure (3a) we observe that the invariant tori and the resonance structure have been destroyed and the elliptic fixed point became a point attractor. Figure (3b) shows the amplification of the neighborhood of this attractor. We started the same ensemble of initial conditions used in figures (2) and we observed that the dynamics is driven toward this attractor, which has velocity  $\sim 0.20$ . So, it is expected that the mean velocity of the ensemble of initial conditions, started with low velocities, be higher than the non-dissipative counterpart. Figure (3c) confirms that prediction, the mean velocity saturated at  $\sim 0.167$ , what implies in a gain of energy of approximately 67% in comparison with the non-dissipative case. This value of the restitution coefficient is not the only possibility to observe this energy gain. Figure (3d) presents a plot for a range of weak dissipation  $e \in [1.0, 0.999]$ , for which this is observed, however the extreme is at  $e \sim 0.9999$ .



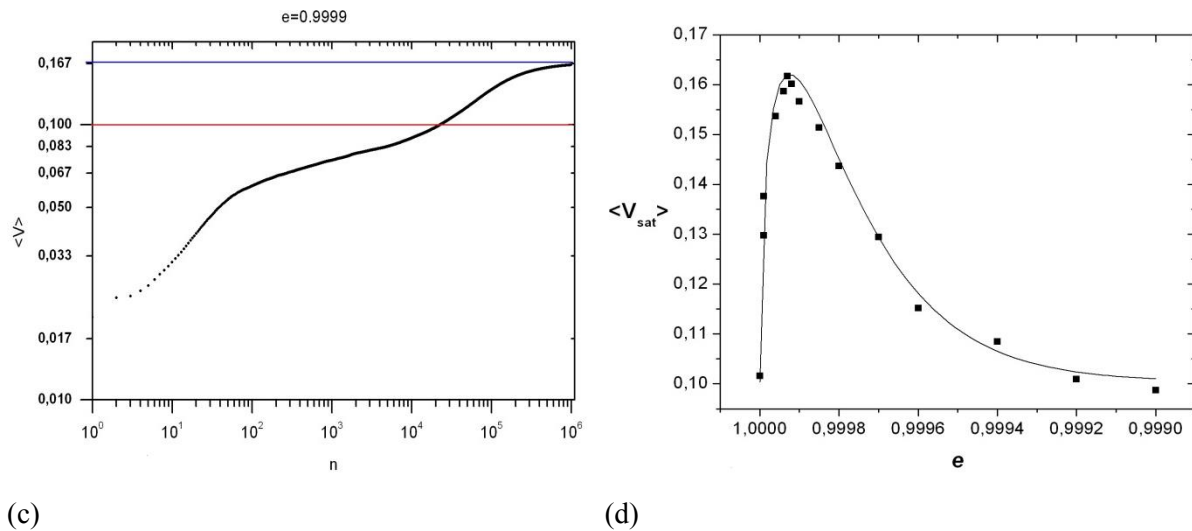


**Figure 3.** Dissipative case, in (a), (b) and (c)  $e=0.9999$ . In a) it is presented the energy phase plane with a point attractor at velocity  $\sim 0.20$ . In b) we see an enlargement around this point attractor. In c) the mean velocity of the same ensemble used in figure (2) converges to the velocity  $\sim 0.167$  (blue line). The red line corresponds to the non-dissipative case. In d) it is shown a range of restitution values for which the particle can gain energy. The peak is at  $\sim 0.9999$ .

We consider now the limit of very strong dissipation. We also set  $\omega = 1$  and  $\phi = 0$ . Figure (4) shows the results we have obtained. In figure (4a) we plot the energy phase plane for the non-dissipative case, which has some similarity with the one of figure (2a), however now we will keep our attention to the elliptic fixed point at  $-V\eta \approx 0.065$  and  $\varphi \approx 0.50$ . In figure (4b) we set  $e = 0.8671$  and we observe the coexistence of a chaotic attractor and a point attractor originated from the elliptic fixed point cited above. We plot the stable (black) and the unstable (red) manifolds of the saddle point (S) originated from the unstable fixed point, partner of the stable one in observation. The upper unstable manifold follows toward the attractive fixed point while the bottom one defines the chaotic attractor. The branches of the stable manifold generate the boundaries of the attractive fixed point, splitting the initial conditions which follow toward the stable focus, from those one heading for the chaotic attractor. We call this regime as *before the crisis*. We decrease slightly the restitution coefficient to  $\gamma = 0.8651$ , what implies in the collision of the stable manifold, which defines the border of the chaotic attractor, with the unstable manifold. These intersections are represented by arrows in figure 4(c). From this value of the restitution coefficient, the basin of attraction of the chaotic attractor, and the chaotic attractor, do not exist any longer, because a boundary crisis occurred. We observe in the place of the chaotic attractor a chaotic transient, which corresponds to the interval of time the initial conditions, departing from the region where there was the chaotic attractor, are captured by the attractive fixed point. We call this regime as *after the crisis*. In figure (4d) we plot the average velocities of an ensemble the 500 initial conditions started with  $-v_\eta = 0.02$  and  $\varphi \in [0, 4\pi]$  for the following three cases: i) the non-dissipative case, with  $\gamma = 1$ ; ii) before the crisis, with  $\gamma = 0.8671$  and iii) after the crisis, with  $\gamma = 0.8651$ . The values of the mean energies after  $5 \times 10^6$  iterations are  $5.69 \times 10^{-2}$ ,  $2.51 \times 10^{-2}$  and  $6.55 \times 10^{-2}$  respectively for the case ii) and iii). Figures (4a), (4b), (4c) and (4d) are authorized to be reproduced from Phys. Rev. E84 (2011) 036204, whose DOI is 0.1103/PhysRevE.84.036204, by the American Physical Society through the license number 3607680086928.



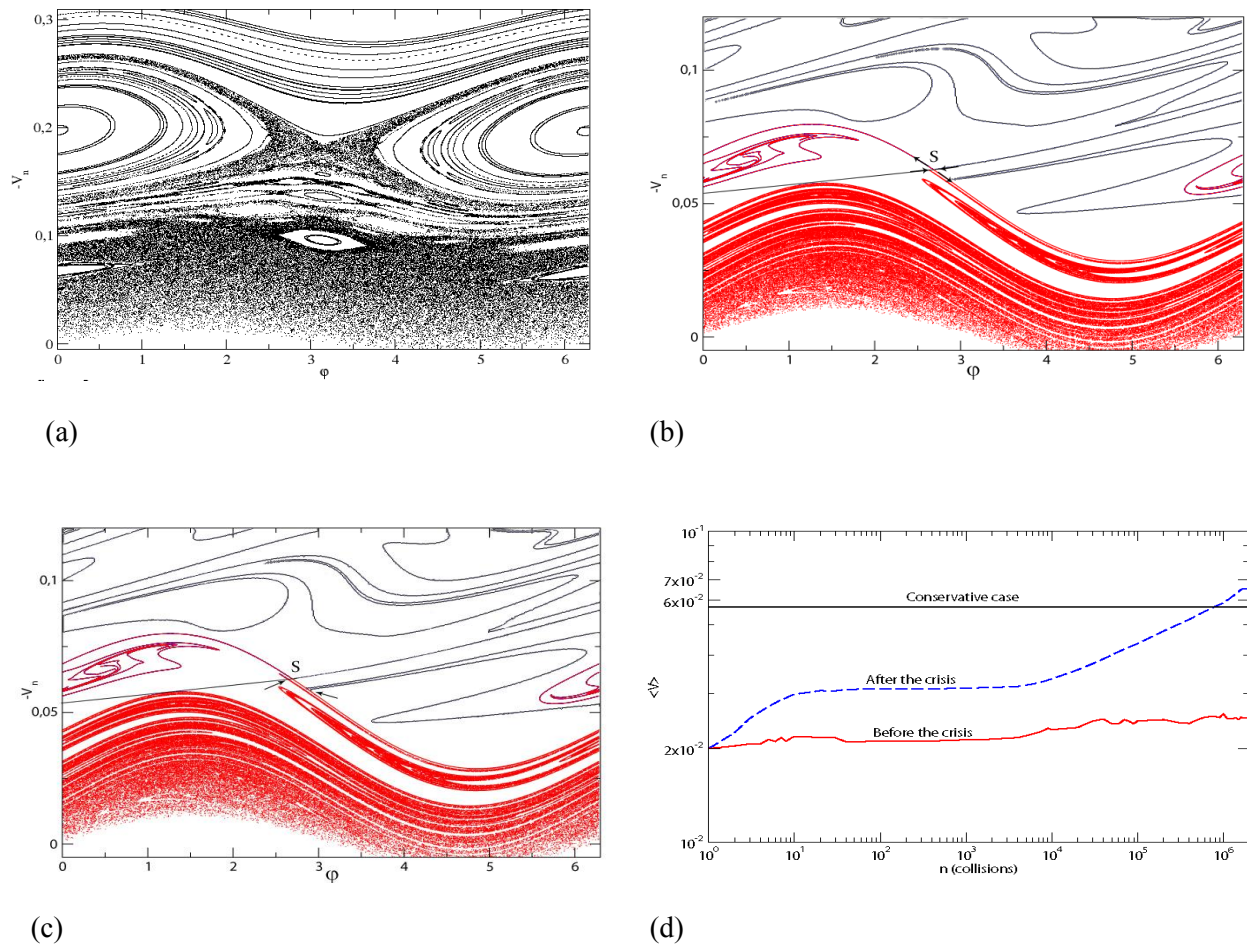


**Figure 4.** a) Energy phase plane for the non-dissipative scenario. Strong dissipation: b)  $e=0.8671$ , before the crisis and c)  $e=0.8651$ , after the crisis; d) the mean velocities for the cases: non-dissipative (black), before (red) and after (blue) the crisis.

We observe that even in the regime of strong dissipation, the particles that started with low velocities attained values of energy that are higher than the ones of the non-dissipative configuration. The responsible mechanism for that energy growth is a boundary crisis that destroyed the chaotic attractor and has driven the particles toward the point attractor, which has higher velocity than the chaotic attractor.

#### 4. Conclusion

In this work we summarize two mechanisms for particles gain energy from the dissipation in two opposite regimes of dissipation intensity. In the limit of weak dissipation, a point attractor is created in the energy phase space with velocity higher than the average velocity of the non-dissipative dynamics. So, an ensemble of particles with low initial velocities is driven toward the point attractor and in the average these particles gain energy after the introduction of dissipation. In the limit of strong dissipation, there are two attractors, a chaotic and a point one. The velocity of the point attractor is higher than the velocity of the chaotic attractor. A boundary crisis occurs in the system and destroys the chaotic attractor leading to a chaotic transient. The trajectories that were travelling in the chaotic

attractor are driven to the point attractor and again they gain energy from the increase of the dissipation intensity. These results have been obtained from a specific model, the breathing annular billiard, however there is no loss of generality in this approach and the ideas can be applied in any system that fulfils the conditions here explained. It is worth noting that all particles that start with initial velocities higher than the velocity of the point attractor, will lose energy.

### Acknowledgement

I thank the Brazilian scientific agency, São Paulo Research Foundation-Fapesp for financial support through the grant 2014/00334-9.

### References

- [1] Ozorio de Almeida A M 1990 *Hamiltonian Systems Chaos and Quantization* (Cambridge: Cambridge Univertisy Preess)
- [2] Grebogi C, Ott E and Yorke J A 1982 *Phys. Rev.Lett.* **48** 1507
- [3] Saitô N, Hirroka H, Ford J, Vivaldi F and Wilker G H 1982 *Physica D* **5** 273
- [4] Bohigas O, Boosé D, Egydio de Carvalho R and Marvulle V 1993 *Nucl. Phys. A* **560** 197
- [5] Egydio de Carvalho R, Souza F C and Leonel E D 2006 *Phys. Rev. E* **73** 066229
- [6] Egydio de Carvalho R, Souza F C and Leonel E D 2006 *J. Phys A* **39** 3561
- [7] Egydio de Carvalho R, Abud C V and Souza F C 2008 *Phys. Rev. E* **77** 036204
- [8] Egydio de Carvalho R and Abud C V 2011 *Phys. Rev. E* **84** 036204